Water Oxidation

DOI: 10.1002/anie.201408795

Catalytic Water Oxidation by Ruthenium(II) Quaterpyridine (qpy) Complexes: Evidence for Ruthenium(III) qpy-*N,N‴*-dioxide as the Real Catalysts[**]

*Yingying Liu, Siu-Mui Ng, Shek-Man Yiu, William W. Y. Lam, Xi-Guang Wei, Kai-Chung Lau, and Tai-Chu Lau**

Abstract: *Polypyridyl and related ligands have been widely used for the development of water oxidation catalysts. Supposedly these ligands are oxidation-resistant and can stabilize high-oxidation-state intermediates. In this work a series of ruthenium(II) complexes* $[Ru(qpy)(L)_2]^{2+}$ *(qpy = 2,2′:6′,2″:6″,2‴-quaterpyridine; L = substituted pyridine) have been synthesized and found to catalyze* Ce^{IV}*-driven water oxidation, with turnover numbers of up to 2100. However, these ruthenium complexes are found to function only as precatalysts; first, they have to be oxidized to the qpy-N,N‴-dioxide (ONNO) complexes* $[Ru(ONNO)(L)_2]^{3+}$ *which are the real catalysts for water oxidation.*

The four-electron oxidation of H_2O to O_2 is a key process in natural and artificial photosynthesis,[1–3] and in recent years there have been considerable efforts in designing robust catalysts for this very important and complicated process.[4,5] Since the discovery of the first water oxidation catalyst (WOC), $[(bpy)_2(H_2O)Ru^{III}ORu^{III}(OH_2)(bpy)_2](ClO_4)_4$ (the "blue dimer", bpy = 2,2′-bipyridine), by Meyer et al. in 1982,[6a] a variety of ruthenium WOCs bearing pyridine-type ligands have been reported.[6–11] Most ruthenium WOCs contain at least an aqua ligand or a labile ligand that can be replaced by water; the aqua complexes undergo proton-coupled electron transfer to generate active Ru=O species. There are also a few six-coordinate ruthenium WOCs that bear only substitution-inert ligands but may form a seven-coordinate Ru=O active intermediate.[7b,8a,12] A notable example is $[Ru(bda)(L)_2]$ (bda = 2,2′-bipyrdine-6,6′-dicarboxylate, L = pyridine and derivatives) reported by Sun et al., which can catalyze water oxidation with a high turnover frequency (TOF) of 300 s^{-1} and turnover number (TON) above 50 000.[8c,d]

We recently discovered that a cobalt(II) complex bearing the 2,2′:6′,2″:6″,2‴-quaterpyridine (qpy) ligand is an efficient catalyst for both water oxidation and reduction.[13] Inspired by the work of Sun et al. we wanted to prepare six-coordinate ruthenium complexes based on qpy and pyridine ligands. Qpy is known to form metal complexes in *trans* configuration with a relatively large N-M-N bite angle,[14] hence it may be possible to form a seven-coordinate M=O species. We describe herein the synthesis and catalytic water oxidation by a series of ruthenium(II) complexes $[Ru(qpy)(L)_2]^{2+}$ (Scheme 1). Polypyridyl ligands coordinated to ruthenium are generally believed to be reasonably stable under water oxidation conditions. However, we provide evidence that in catalytic water oxidation using $(NH_4)_2[Ce(NO_3)_6]$ (CAN) as terminal oxidant, the qpy ligand in $[Ru(qpy)(L)_2]^{2+}$ is first oxidized to a qpy-*N,N‴*-dioxide (ONNO). The resulting complex $[Ru(ONNO)(L)_2]^{3+}$ is the real catalyst for water oxidation.

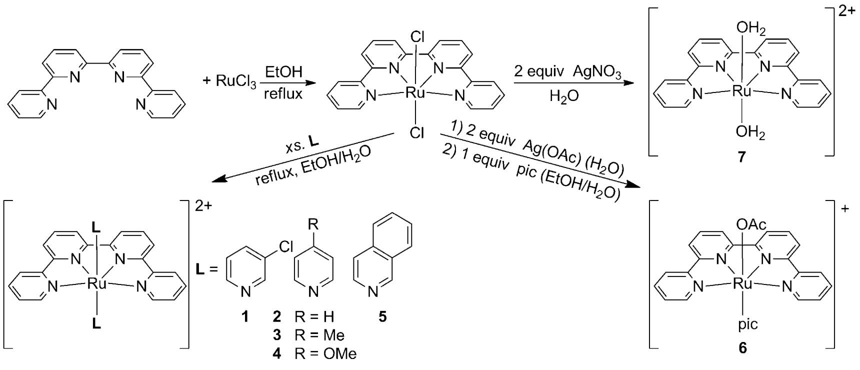

Scheme 1. Synthetic routes for ruthenium complexes **1**–**7**.

The synthesis of the ruthenium complexes is summarized in Scheme 1; complex **7** has been reported by Che et al.[14] The structures of **3**, **4**, and **5** have been determined by X-ray crystallography. In **3**, the ruthenium center adopts a distorted octahedral geometry with the equatorial positions occupied by the planar qpy ligand, and the axial positions by two

---

[*] Y. Liu, Dr. S. M. Ng, Dr. W. W. Y. Lam, X. G. Wei, Dr. K. C. Lau, Prof. T. C. Lau
Department of Biology and Chemistry
and
Institute of Molecular Functional Materials
City University of Hong Kong
Tat Chee Avenue, Kowloon Tong, Hong Kong (China)
E-mail: bhtclau@cityu.edu.hk

[**] This work was supported by the Hong Kong University Grants Committee (AoE/P-03-08), the Shenzhen Science and Technology Research Grant (JCYJ20120613115247045), and the Shenzhen Research Institute, City University of Hong Kong.

Supporting information for this article is available on the WWW under http://dx.doi.org/10.1002/anie.201408795.

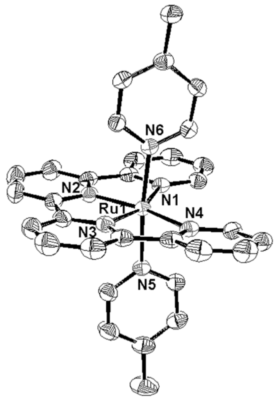

Figure 1. ORTEP plot of **3**. Thermal ellipsoids are drawn at 50% probability; anions, solvent, and hydrogen atoms are omitted for clarity.

picoline ligands (Figure 1 and Tables S1 and S2). The distances of the ruthenium center to the two outer pyridyl N atoms (Ru1–N1 2.132 Å, Ru1–N4 2.129 Å) are significantly longer (by 0.18 Å) than those to the inner pyridyl N atoms (Ru1–N2 1.946 Å, Ru1–N3 1.952 Å), due to considerable strain in the planar coordination mode of the qpy ligand. The X-ray structures of **4** and **5** are similar to that of **3** (Figure S1 and Tables S1 and S2).

Complexes **1**–**5** exhibit a reversible redox wave in cyclic voltammetry (CV) in H_2O/CH_3CN (3:1 v/v) at pH 1, which is assigned to the $Ru^{III/II}$ couple (Table 1, Figure S2). The CV of **3** is shown in Figure 2. The $E_{1/2}$ values of **1**–**5** are similar to that of $[Ru(bpy)_3]^{3+/2+}$ (1.02 V versus SCE).[15] Complexes with electron-donating groups, such as **3** and **4**, have slightly lower $E_{1/2}$ than those with electron-withdrawing groups, such as **1**.

Table 1: $Ru^{III/II}$ $E_{1/2}$ [V] and catalytic water oxidation data for complexes **1**–**5**.

Complex	$E_{1/2}$ [V] (ΔE [mV])[a]	TON[b]	TOF_{max} [min^{-1}][c]
1	1.11 (58)	219	1.0
2	1.05 (58)	327	1.0
3	1.02 (56)	576	1.5
4	0.99 (56)	707	1.9
5	1.05 (62)	293	4.9

[a] Versus SCE. [b] Ruthenium complexes, 25 μM; CAN, 247 mM; $T = 25$ °C. TON = (mol of O_2)/(mol of catalyst). [c] The maximum TOF is calculated from the initial slope.

Although there is no catalytic current upon scanning to 1.6 V versus SCE in CV, oxygen evolution was readily observed for complexes **1**–**5** in water upon adding CAN (Figure 3 and Table 1). Complex **5** shows the highest TOF (4.9 min^{-1}), but it has a relatively low TON of 290; whereas **4** gives the highest TON of 700. On the other hand, complexes **6** and **7**, which have one and no axial pyridine ligand, respectively, do not show any catalytic activity. By using a lower concentration of 2.5 μM, a TON of 1700 could be achieved for **4** (Table S3). The TON was further increased to 2100 in the presence of 1.2% CF_3CH_2OH (instead of CH_3CN).

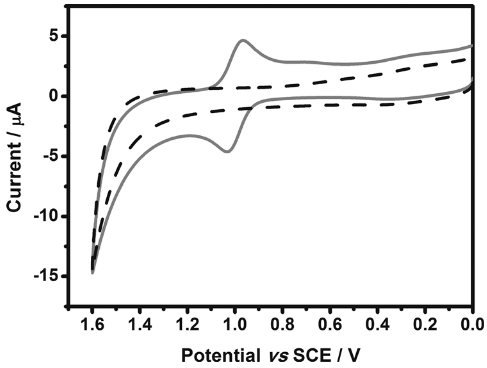

Figure 2. CV of **3** (0.5 mM, solid line) and blank (dashed line) at pH 1 in H_2O/CH_3CN (3:1 v/v). Scan rate = 100 mV s^{-1}.

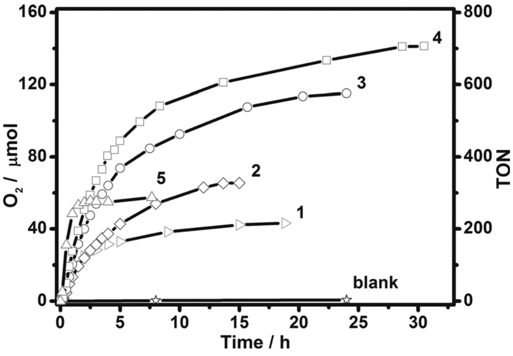

Figure 3. Plots of oxygen evolved and TON versus time for water oxidation by complexes **1**–**5** (25 μM) and CAN (247 mM) in 0.1 M HOTf (8.0 mL) containing CH_3CN (0.1 mL, to enhance solubility) at 25 °C. Oxygen was monitored by GC-TCD (TCD = thermal conductivity detector).

We then tried to detect any intermediates formed during water oxidation by ESI-MS (Figure S3). The MS of **3** in water (pH 2) exhibits the parent peak $[Ru(qpy)(pic)_2]^{2+}$ (pic = 4-picoline) at $m/z = 299$. Upon addition of 2 equiv of CAN, an additional peak at $m/z = 307$ appeared, which may be assigned to $[Ru(qpy)(pic)_2{+}O]^{2+}$. When another 2 equiv of CAN were added, the parent peak disappeared, and a minor peak at $m/z = 315$ appeared, which may be assigned to $[Ru(qpy)(pic)_2{+}2O]^{2+}$. $[Ru(qpy)(pic)_2{+}2O]^{2+}$ became the predominant peak after addition of 8 equiv of CAN (Figure 4). Similar results were found for **1** and **4**. The observation of peaks with one and two additional O atoms are often assigned as oxo and superoxo/peroxo species, respectively, that is, $[Ru(qpy)(pic)_2(O)]^{2+}$ and $[Ru(qpy)(pic)_2(O_2)]^{2+}$.

We then attempted to isolate these intermediates. Treatment of **3** with excess CAN (40 equiv) in 0.1 M HOTf followed by the addition of NH_4PF_6 resulted in the formation of an orange compound **8**$[PF_6]_3$ in 50% yield. The X-ray structure of **8**$[PF_6]_3$ (Figure 5) shows that it consists of the complex $[Ru(ONNO)(pic)_2]^{3+}$ (ONNO = 1,1‴-dioxide-2,2′:6′,2″:6″,2‴-quaterpyridine), in which the ONNO ligand is derived from oxidation of the two outer pyridyl groups of the qpy ligand to a *N,N‴*-dioxide. The O1-Ru1-O2 bite angle is 101.86°, which

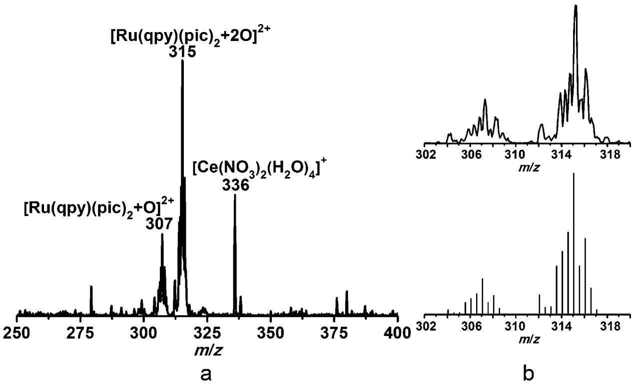

Figure 4. a) ESI-MS of **3**[Cl]$_2$ (1.0 mM) in 0.01 M HNO_3 recorded 20 min after the addition of 8 equiv of CAN. The solution was diluted 10 times before electrospraying. b) The expanded (top) and calculated (bottom) isotopic patterns.

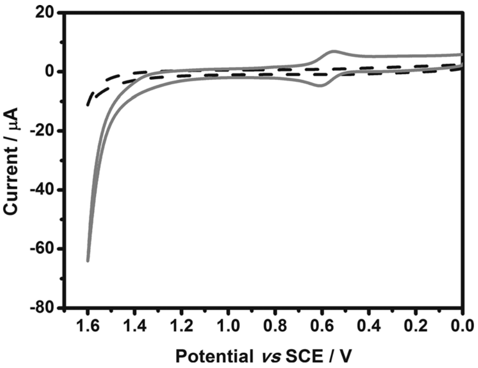

Figure 6. CV of **8** (0.5 mM, solid line) and blank (dashed line) in 0.1 M HOTf. Scan rate = 100 mV s^{-1}.

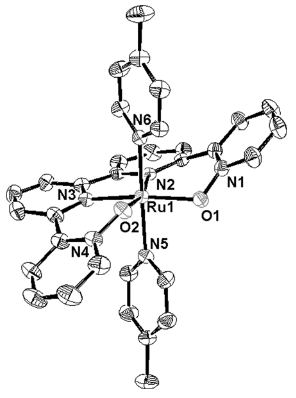

Figure 5. ORTEP plot of **8**. Thermal ellipsoids are drawn at 50% probability; anions, solvent, and hydrogen atoms are omitted for clarity.

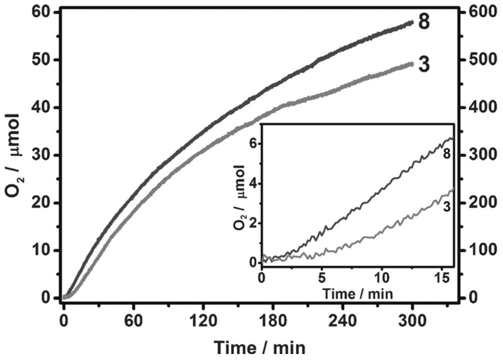

Figure 7. Plots of oxygen evolved and TONs versus time by 20 µM of **3** and **8** in 0.1 M HOTf (4.8 mL) and CH_3CN (0.2 mL) containing CAN (200 mM) at 25 °C. Inset shows oxygen evolution curves in the first 15 min.

is larger than the ideal value of 90° for an octahedral complex, but is much smaller than the N1-Ru1-N4 angle of 120.89° in **3**. The CV of **8** in H_2O (pH 1) shows a reversible $Ru^{III/II}$ couple at 0.58 V versus SCE, which is lower than that of its precursor **3** by 0.44 V, in accordance with the replacement of the qpy ligand in **3** by the less π-accepting ONNO ligand in **8**. In contrast to **3**, there is a catalytic current for **8** in CV with an onset potential at around 1.3 V versus SCE (Figure 6). When oxidation of **3** was carried out using 10 equiv instead of 40 equiv of CAN, the CV of the resulting complex **8** contains a minor peak at 0.78 V, which is most likely due to the first oxidation product $[Ru(NNNO)(pic)_2]^{3+}$ (Figure S4). Based on these results, the $[Ru(qpy)(pic)_2{+}O]^{2+}$ and $[Ru(qpy)(pic)_2{+}2\,O]^{2+}$ peaks in the MS in Figure 4 should arise from $[Ru(NNNO)(pic)_2]^{3+}$ and $[Ru(ONNO)(pic)_2]^{3+}$, respectively, and not from any Ru(O) or Ru(O_2) species.

The isolation of the Ru–ONNO complex **8** raises the interesting question of whether it is a WOC or merely a byproduct. To answer this question, catalytic water oxidation by **8** was studied and compared with the reaction catalyzed by **3**. Oxygen evolution was continuously monitored using an Ocean Optics oxygen sensor (Figure 7). For **8**, O_2 evolution occurred within 1 min after the addition of CAN, whereas for **3** an induction period of about 5 min was observed under the same reaction conditions. After the induction period, the rate of O_2 evolution by **3** was comparable to that of **8**. The observed induction period for **3** may be interpreted as arising from its initial oxidation to the *N,N‴*-dioxide complex **8**, which is the real catalyst for water oxidation. This notion is also supported by the observation that **8**, but not **3**, shows a catalytic current in CV.

If complex **8** is the real catalyst, then there is the issue of whether the O atoms in O_2 come from the ONNO ligand, that is, ONNO→NNNN+O_2, or directly from H_2O, and to answer this question we performed ^{18}O-labeling experiments. We first prepared ^{18}O-labeled **8**, $[Ru(^{18}ONN^{18}O)(pic)_2]^{3+}$, by reacting **3** with CAN in $H_2{}^{18}O$. A single turnover experiment was then performed by treating [^{18}O]-**8** with 4 equiv of CAN in $H_2{}^{16}O$ under argon in 0.1 M HOTf. The O_2 generated (0.69 µmol, yield 58%) was found to be exclusively $^{16}O^{16}O$, as analyzed by GC-MS (Figure S5). This means that all O atoms in O_2 came directly from water. Moreover, the ESI-MS of the solution after water oxidation shows only ^{18}O-containing ruthenium species, the predominant peak is $[Ru(^{18}ONN^{18}O)(pic)_2]^{2+}$ ($m/z = 317$). A similar mass spectrum was obtained using 16 equiv of CAN (Figure 8). The ESI-MS results again show that the O atoms in O_2 did not come from the ONNO ligand.

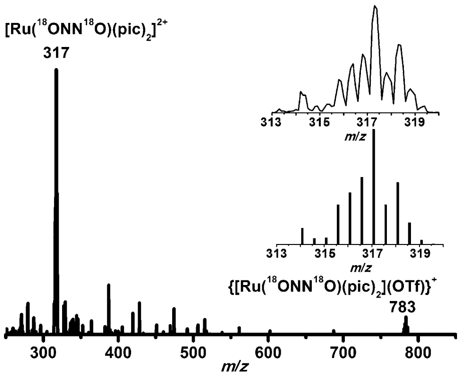

Figure 8. ESI-MS of ^{18}O-labeled **8** after reacting with 16 equiv of CAN in 0.1 M HOTf. Insets show the expanded (top) and calculated (bottom) isotopic patterns.

It also reveals that **8** does not exchange its O atoms with H_2O during the catalysis.

Kinetic studies for water oxidation by **8**/CAN were performed by monitoring the amount of evolved O_2 as a function of time (Figure S6). The initial rate shows a linear dependence on [**8**], and a first-order rate constant of 2.1 min^{-1} (25 °C) was obtained from the slope. This result suggests that catalytic water oxidation by **8** probably occurs through a "water nucleophilic attack" mechanism.[6b,9a] We propose that the active intermediate is a seven-coordinate ruthenium(V) oxo species, $[Ru(O)(ONNO)(L)_2]^{2+}$, by analogy to the WOC $[Ru(bda)(L)_2]$.[8c] DFT calculations have been performed, which indicate that the seven-coordinate ruthenium(V) oxo species is stable with a Ru=O distance of 1.767 Å (Figure S7).

Polypyridyl ligands are widely used in WOCs and it is generally believed that these ligands are reasonably oxidation-resistant. We have demonstrated that ruthenium(II) complexes bearing a quaterpyridine ligand function only as precatalysts for water oxidation. In the presence of CAN these complexes are readily oxidized to the qpy-*N*,*N'''*-dioxide complexes $[Ru(ONNO)(L)_2]^{3+}$, which are the real WOCs.

Received: September 4, 2014

Keywords: density functional calculations · homogeneous catalysis · polypyridyl ligands · ruthenium complexes · water oxidation

---

[1] H. B. Gray, *Nat. Chem.* **2009**, *1*, 7.

[2] J. J. Concepcion, R. L. House, J. M. Papanikolas, T. J. Meyer, *Proc. Natl. Acad. Sci. USA* **2012**, *109*, 15560 – 15564.

[3] D. G. Nocera, *Acc. Chem. Res.* **2012**, *45*, 767 – 776.

[4] A. Llobet, *Molecular Water Oxidation Catalysts*, Wiley, Hoboken, **2014**.

[5] X. Liu, F. Wang, *Coord. Chem. Rev.* **2012**, *256*, 1115 – 1136.

[6] a) S. W. Gersten, G. J. Samuels, T. J. Meyer, *J. Am. Chem. Soc.* **1982**, *104*, 4029 – 4030; b) J. J. Concepcion, J. W. Jurss, J. L. Templeton, T. J. Meyer, *J. Am. Chem. Soc.* **2008**, *130*, 16462 – 16463; c) J. J. Concepcion, J. W. Jurss, M. K. Brennaman, P. G. Hoertz, A. O. T. Patrocinio, N. Y. M. Iha, J. L. Templeton, T. J. Meyer, *Acc. Chem. Res.* **2009**, *42*, 1954 – 1965; d) J. J. Concepcion, M.-K. Tsai, J. T. Muckerman, T. J. Meyer, *J. Am. Chem. Soc.* **2010**, *132*, 1545 – 1557.

[7] a) R. Zong, R. P. Thummel, *J. Am. Chem. Soc.* **2005**, *127*, 12802 – 12803; b) H.-W. Tseng, R. Zong, J. T. Muckerman, R. Thummel, *Inorg. Chem.* **2008**, *47*, 11763 – 11773.

[8] a) L. Duan, A. Fischer, Y. Xu, L. Sun, *J. Am. Chem. Soc.* **2009**, *131*, 10397 – 10399; b) L. Tong, L. Duan, Y. Xu, T. Privalov, L. Sun, *Angew. Chem. Int. Ed.* **2011**, *50*, 445 – 449; *Angew. Chem.* **2011**, *123*, 465 – 469; c) L. Duan, F. Bozoglian, S. Mandal, B. Stewart, T. Privalov, A. Llobet, L. Sun, *Nat. Chem.* **2012**, *4*, 418 – 423; d) L. Duan, C. M. Araujo, M. S. G. Ahlquist, L. Sun, *Proc. Natl. Acad. Sci. USA* **2012**, *109*, 15584 – 15588.

[9] a) X. Sala, S. Maji, R. Bofill, J. García-Antón, L. Escriche, A. Llobet, *Acc. Chem. Res.* **2014**, *47*, 504 – 516; b) S. Neudeck, S. Maji, I. López, S. Meyer, F. Meyer, A. Llobet, *J. Am. Chem. Soc.* **2014**, *136*, 24 – 27.

[10] S. Masaoka, K. Sakai, *Chem. Lett.* **2009**, *38*, 182 – 183.

[11] a) D. J. Wasylenko, C. Ganesamoorthy, B. D. Koivisto, M. A. Henderson, C. P. Berlinguette, *Inorg. Chem.* **2010**, *49*, 2202 – 2209; b) D. J. Wasylenko, R. D. Palmer, C. P. Berlinguette, *Chem. Commun.* **2013**, *49*, 218 – 227.

[12] T.-T. Li, Y. Chen, F.-M. Li, W.-L. Zhao, C.-J. Wang, X.-J. Lv, Q.-Q. Xu, W.-F. Fu, *Chemistry* **2014**, *20*, 8054 – 8061.

[13] C.-F. Leung, S.-M. Ng, C.-C. Ko, W.-L. Man, J. Wu, L. Chen, T.-C. Lau, *Energy Environ. Sci.* **2012**, *5*, 7903 – 7907.

[14] C.-W. Chan, T.-F. Lai, C.-M. Che, *J. Chem. Soc. Dalton Trans.* **1994**, 895 – 899.

[15] A. Juris, V. Balzani, F. Barigelletti, S. Campagna, P. Belser, A. von Zelewsky, *Coord. Chem. Rev.* **1988**, *84*, 85 – 277.